CHAPTER VI

GEOMORPHOLOGY AND STRUCTURE

VI.1 Introduction

The Eastern Desert is bounded by the Nile valley in the west and by Suez Canal, the Gulf of Suez and the Red sea in the east. It occupies a substational portion of Egypt, with an area greater than 223,000 Sq. Km (21%)of the total area of the country. The Eastern Desert contain a mountain chain known as Red sea Mountains formed of igneous rocks, running parallel to Red sea. Neighboring the Red sea Mountains on the north and west are dissected plateaus formed from sedimentary rocks e.g. El Galala El Baharia, El Galala El Qibliya and Gabal Ataqa. Northern Eastern Desert comprises plateaux, cuestas, mesas and hills (Abdallah 1993).

VI.2 Geomorphology the study area

The study area is a wide depression falling between the southern scarps of Gabal Ataqa on the north, and the northern scarp of Gabal El-Galala El-Bahariya on the south. It is bounded by the Gulf of Suez, on the east and to the west it rises gradually until it merges into the central plateau forming the northern part of the Eastern Desert of Egypt. Topographic highs are made up of hard Lower and Middle Eocene limestone beds while the topographic lows are filled with the soft rocks ranging in age from Late Eocene to Recent. The study area comprises the following main units:

VI.2.1 The Coastal Plain Unit

The Gulf of Suez Coastal Plain is restricted to the western shore areas of the Gulf of Suez. It is a narrow strip with a width that changes from a few meters in the area east of the El Galala

El Bahariya to about 3 km in the downstream areas of Wadis Ghoweiba and Hagoul. Lithologically, the surface of this plain is covered by sands, gravels, salt marsh deposits, playas, and sabkhas of Quaternary age. It mostly has very limited elevation above the Gulf of Suez water level.

Four major wadies downstream into the coastal plain and to the Gulf of Suez, these are from north to south; wadi Hagoul, wadi El-Bada, wadi El-Akheider and waid Ghoweibba. The plaines of these wadies are essentially structurally controlled (Sadek, 1926). El-Ghoweibba plain is represented by the graben enclosed between the South Akheider Plateeau from the north and the major E – W faults that form the northerly major escarpment of the North Galala from the south. The surface of this plain is characterized by several raised beaches, sabkhas, and the natural Ain Sukhna spring.

VI.2.2 The High land unit

Gabal Ataqa, Northern Galala, and the plateaus, which occupy respectively the central, west – central and some northwesten parts of the area are the highest lands in the study area and consider the upstreams of most drainages in the area of study. There are 3 main valleys separating four plateaux; Wadi Hagul separates between Gabal Attaqa and Gabals Kahalyia-Um Zeita plateau, Wadi El-Bada separates between Kahalyia-um Zeita-Abu Treifa Plateau and Ramliya-Gabal Akheider plateau and Wadi Ghoweiba separates between Ramliya-Gabal Akheider plateau and El-Galala El-Bahariya.

A - Gabal Ataqa

The Ataqa mountain is a huge cuesta-like feature that occupies the northeastern margin of the northern Eastern Desert area. It is a triangular in -shape and is capped by hard Middle Eocene limestone beds. Its sides are fault-controlled except the southwestern side which is a dip slope. The elevation of its surface varies from about 730m to about 300m the down dip slope side. The elevation of the northern scarp from about 680m in the east to about 300m in the west where it merges westward into the Wadi Hagoul plain that borders the northern part the El Qattamia-Abu Treifiya Plateau.

B - Gabal northern Galala

One of the topographical features in the northern part of the Gulf of Suez is the great massive block known as El-Galala El-Bahariya. It extends as a high plateau bounded by scarps that rise as sheer vertical cliffs from the boundary of the Gulf, and is flanked on the north and south by the wide depressions of Ghoweibba and Araba respectively. The highest point of 977 meters above sea level appears at its eastern end. El-Galala plateau considers the tributaries to the most wadies downstream in wadi Ghoweibba. Middle Eocene rocks cover the top of Northern Galala plateau (Said, 1990) while the Paleozoic and Mesozoic rocks are exposed along the eastern scarp facing the Gulf of Suez.

VI.2.3 The Low Lying Hill Unit

The hilly unit is mainly covered by the Upper Eocene, Oligocene and Miocene rocks. It occupies three main localities in the northern, central and southwestern parts of

the study area, bounding the high landmasses. The first, northern locality has an east – northeasterly direction bordering the main trunk of Waid El-Bada. It is made up mainly of Upper Eocene clays and sandy limestones, and Oligocene gravels. The second on is bounding the central plateau of Gabal Akheider from the east. It is dominated by Upper Eocene and Miocene clastics, which are structurally controlled. Their strip has a general slope, coinciding with the dip, towards the Gulf of Suez (Sadek, 1926).

VI.2.4 The drainage pattern

The study area is crossed by several wadis such as Ghoweiba, Bada, Akheider and Hagoul.The Wadi Ghoweib plain occupies the central strip of study area and considered largest and most important drainage. It is bounded from the south by the El Galala El Bahariya Plateau and from the north by Akheider Plateaux. The Plain is filled with soft rocks ranging from Late Eocene to Recent. This Plain has a rectangular shape and covers an area of about 200 km2 (Abdallah 1993). The Wadi Hagoul and Wadi Akheider plain lies NW of the Gulf of Suez. It is bounded from the NE by the Gabal Ataqa huge cuesta and from the west by the El Qattamia-Abu Treifiya and Akheider plateaux. It has a NW-SE orientation and is fault-controlled. The plain is composed of soft rocks ranging in age from Late Eocene to Quaternary

VI.3 Digital Elevation Model (DEM) Creation

DEMs are digital elevation model data. DEM was originally a term reserved for elevation data provided by the United State Geological Survey, but it is now used to describe any digital elevation data.

The DEM has been created using ERDAS Imagine software 9.1 version (Fig. 74) while the slope and shaded relief maps have been carried out using Arc GIS 9.1 software. The slope of the surface determines the energy of flow. Slope is the maximum rate of change in elevation from each cell. The area shows gentle slope along the shore (Fig. 75), the maximum sloping is clearly on Gabal Ataqa and El Galala plateau. Slope is expressed as percentage or calculated in degrees.

Analytical hillshading is away to determine the hypothetical illuminiation of the surface, (Fig. 76) shows the shaded relief of the study area.

obeikandl.com

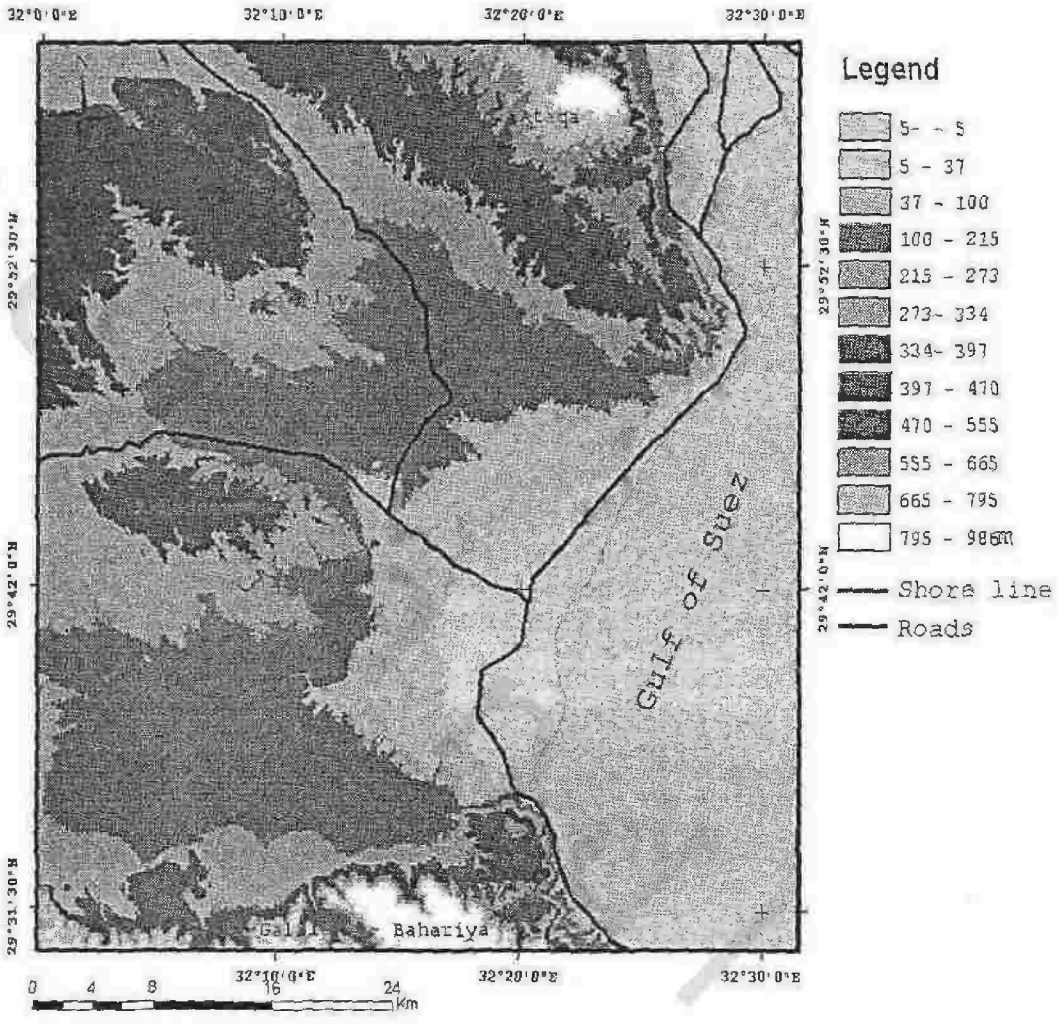

Figure (74): Digital Elevation Model (DEM) of the study area.

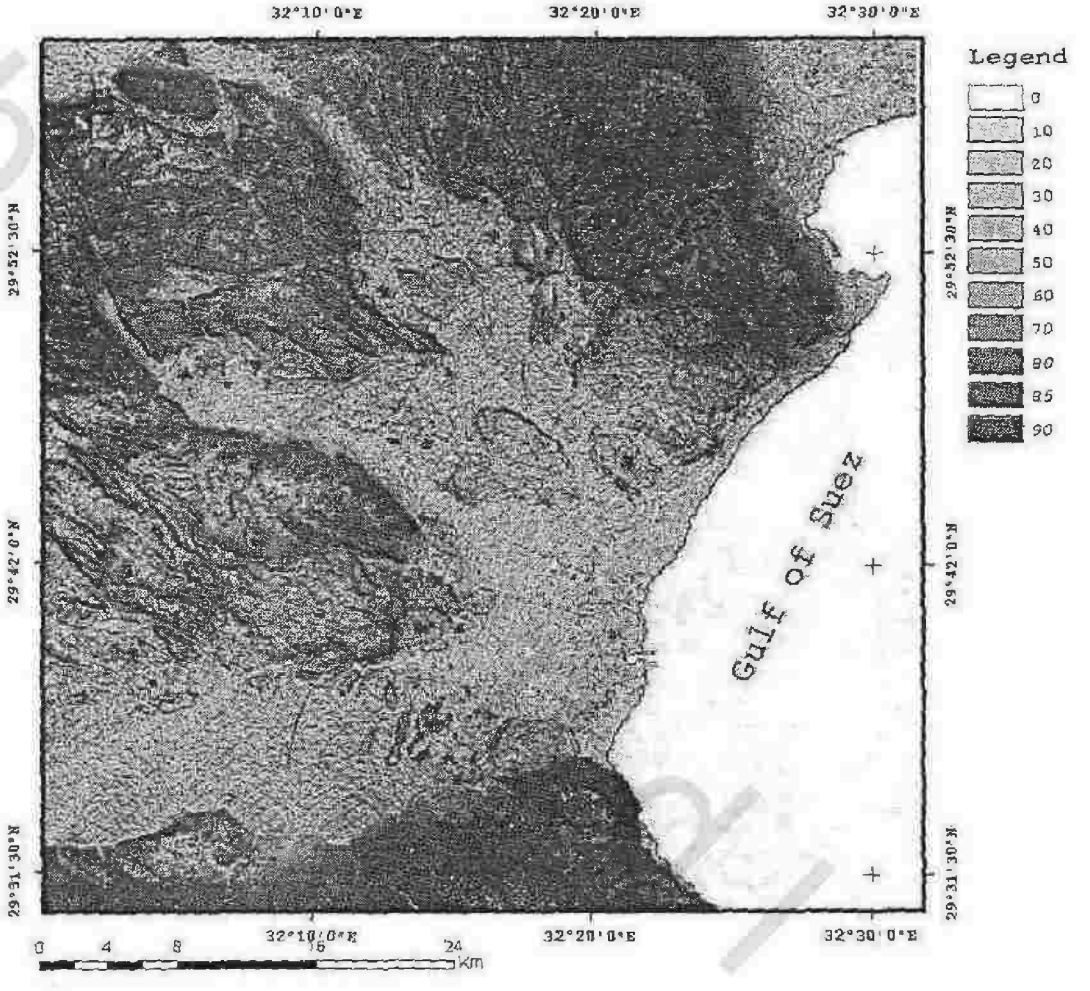

Figure (75): Slope map of the study area.

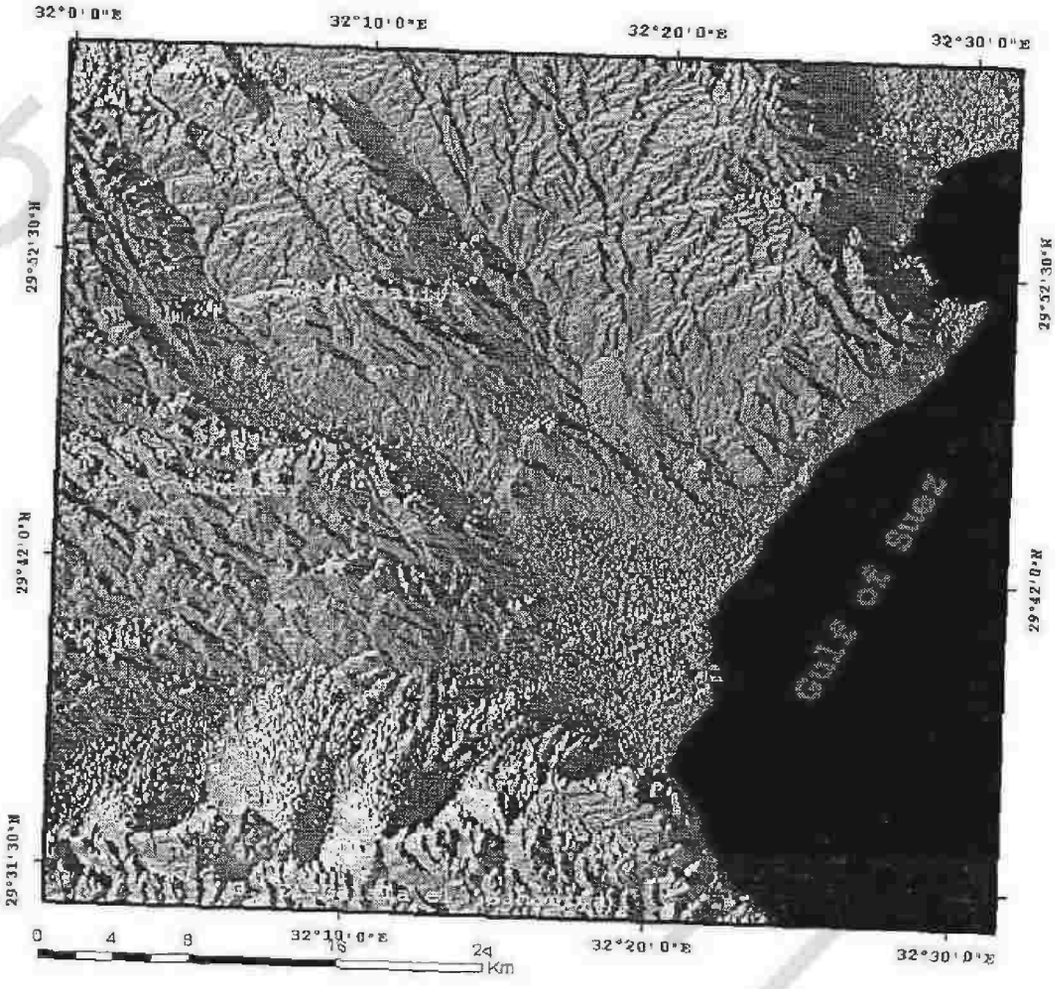

Figure (76): Shaded relief map of the study area.

VI. 4. Tectonic setting in the studied area:

The area is located along the north western side of the Gulf of Suez, which is affected by the Red Sea rift tectonics. This rift called as the "Clysmic" rift, after the ancient Roman settlement of Clysma that occupied the present site of the city of Suez (Hume, 1921; Robson, 1971). The Gulf of Suez rift comprises a northwest trending intra-cratonic basin that is separated from the Red Sea by the Aqaba transform fault. The Gulf of Suez rift is bounded on the east by the Sinai massif and on the west by the Red sea hills of the Eastern Desert.

The study area is mainly controlled by faults and limited folds. Safei EL-Din (1988): study the area between Gabal Ataqa and the Northern Galal, showed that there are two main fault sets, which are NW to WNW and E-W. Some faults of the WNW orientation form four E-W elongated fault belts of left-stepped, en echelon, normal faults. These belts are called, from north to south, Gabal Um Zeita, Gabal El Ramliya, Wadi Akheider and Wadi El Shona. He interpreted these fault belts as right-lateral strike slip movement rejuvenated overlying four deep-seated faults that have the same trends.

According to Abdallah (1993) and Sadek (1926) the structural deformation of the study area took place in four tectonic events. These are; from old to young: Early Oligocene event, Late Oligocene-Early Miocene event, early Late Miocene, and post-Miocene event. The first two events are of more drastic deformations than the other two and were responsible for the formation of the main structural and topographic features of the study area and probably other parts of the northern Eastern Desert.

VI. 5. Lineament extraction

One of the main purposes of this technique is to prepare structural map based on the remote sensing data interpretation then compared to the geological, structural map and geophysical trend patterns. A lineament is defined as a linear features or patterns that are visible very well on a remote sensing image. It reflects the geologic structures such as faults or fractures in the form linearly organized elements of the landscape.

A lineament is a mappable linear or curvilinear feature of a surface whose parts align in a straight or slightly curving relationship that may be the expression of a fault. The surface features making up a lineament may be geomorphic (caused by relief) or tonal (caused by contrast differences). Straight stream valleys are typical geomorphic expression of lineaments. Atonal lineaments may be a straight boundary between areas of contrasting tone or a stripe against a background of contrasting tone. Lineaments that coincide with lines of structural offset are called faults (Sabines, 1997).

After tracing all lineaments from the landsat image Fig. (77), their orientations and lengths were determined and measured, then analyzed by preparing histogram for analysis, interpretation and comparison with geologic map Fig. (78).

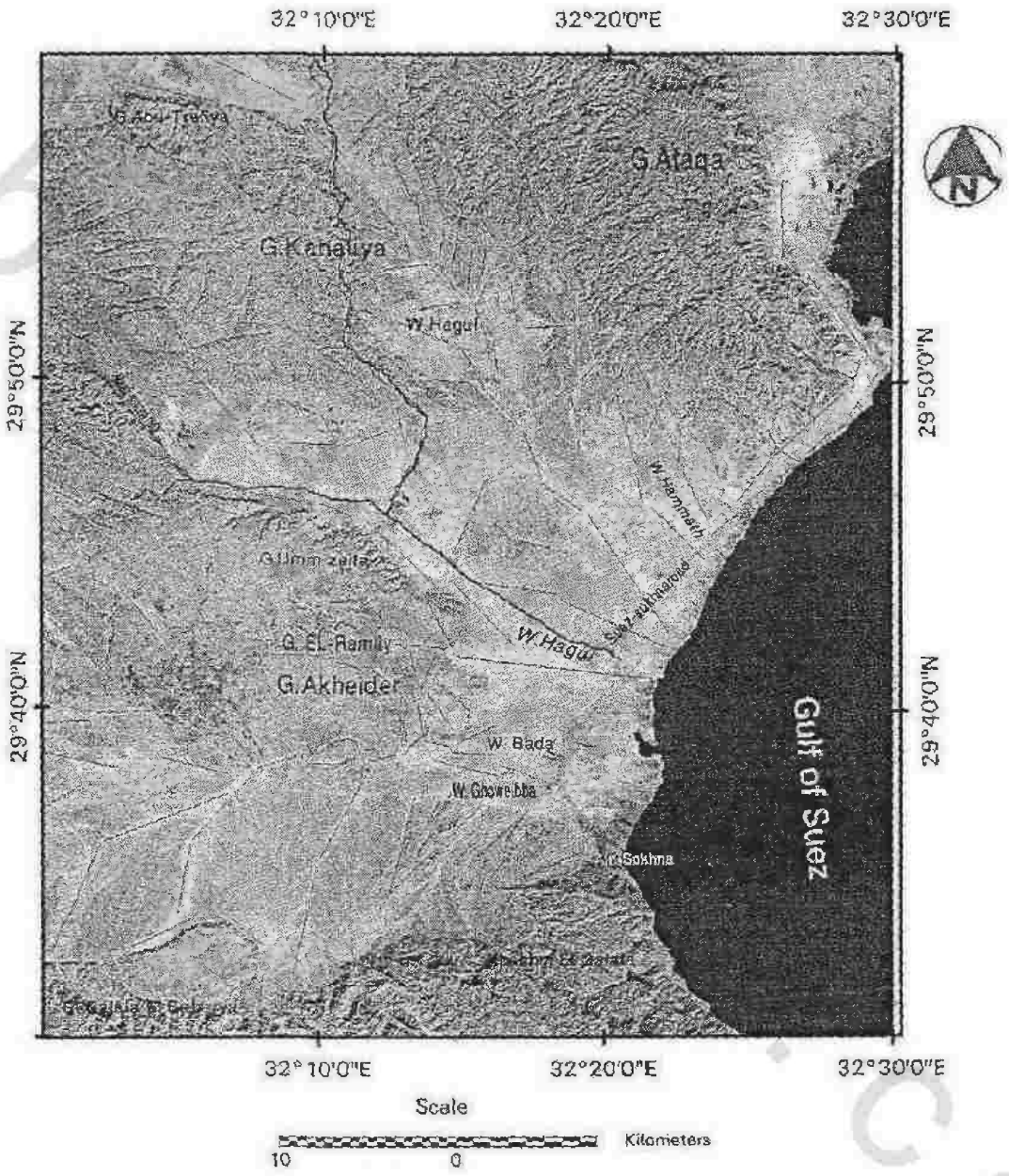

Figure (77): Lineaments map of the study area extracted from the Landsat image.

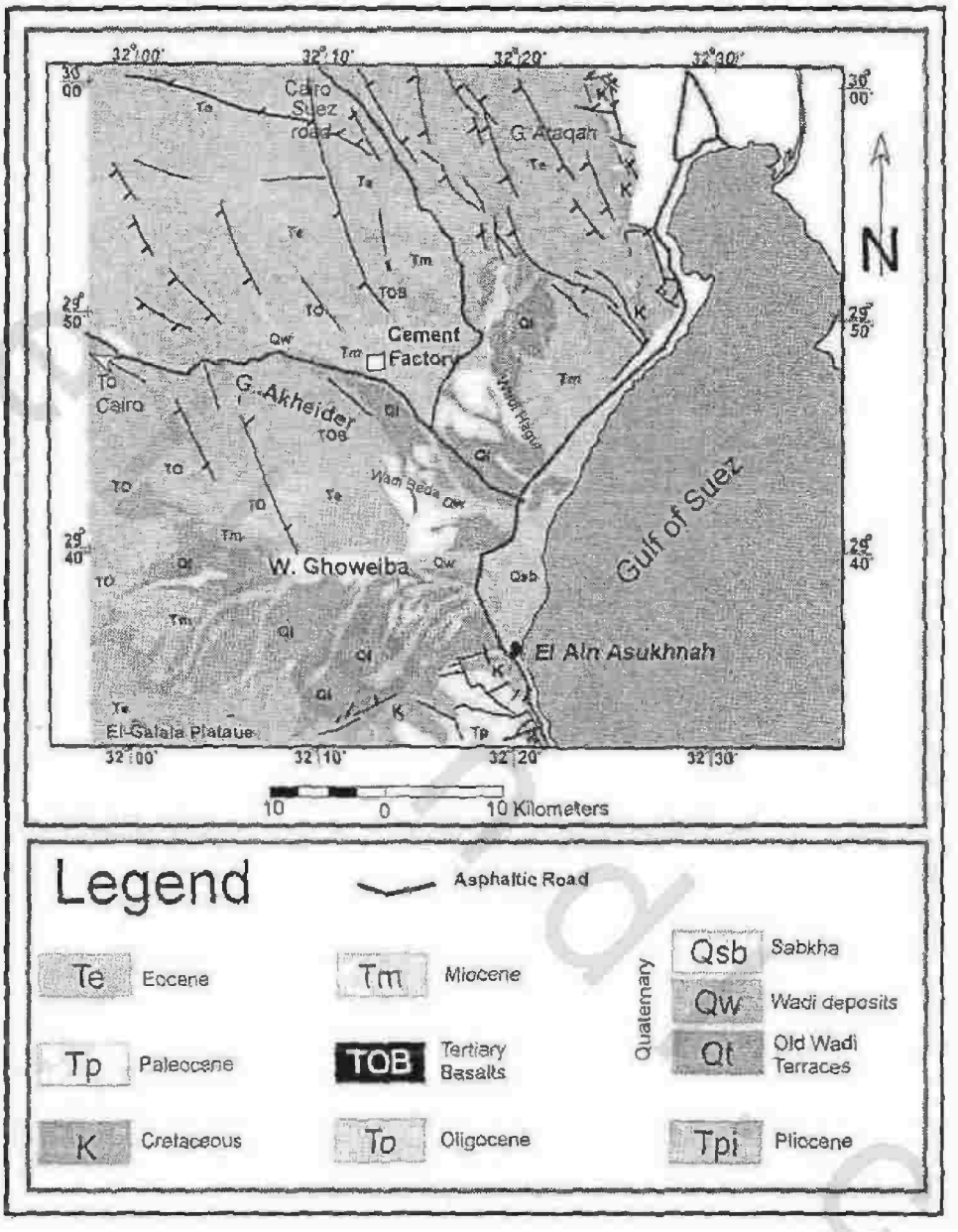

Figure (78) Geological map of the study area (after EGSMA,1999).

Halsey and Gardner (1975) have classified the linear features, recorded on the satellite photographs, of all the Egyptian territories into three major trend groups N 35 W, N15 E, and N 60 E and four minor trends N 40 E, N-S, E-W, and N 60 W.

According to Hassan (2008); there are 586 faults out of 788 affecting the Eocene rocks, which are responsible for the formation of the relief of the study area. These faults divided into three main types, their orientation are NW, NNW and EW. The faults that dissect the Miocene rock units exist in three fault sets which are E-W, NW and NNW, parallel with the sets of faults affecting the Eocene rock units but of short to intermediate lengths and small to slightly intermediate throws less than 100m. Some of the NW oriented faults and the E-W oriented faults are found in the Northern Galala belt, Wadi El Shona-Wadi Ghoweiba belt, and Wadi Akheider belt.

VI. 6 . Lineament analysis

Lineaments are mostly the traces of discontinuities such as bedding planes, faults and fractures with the ground surface. These surface features when properly identified, can usually be assumed to reflect subsurface structures of an area. Thus, the analysis of lineaments not only provides a method for detecting past tectonic trends but also helps in the exploration of minerals, oil, and ground water and the seismic risk for nuclear sites and repository studies as well (Mustafa and Zakir,1996).

The photo lineaments extracted from the landsat image indicates that the area is dominated by four sets of faults. This arranged according to the degree of predominance are the NW, WNW, NNW and NE sets. Each trend of lineaments sets will be

discussed separately as follows:

NW-SE (Gulf of Suez –Red Sea) trend:

The NW oriented faults are characterized by their long lengths, about 23.62% of the total length and 22.52% of the total number of all structural lineaments Table (4) and Fig (79). The NW trend comprises all lineaments trending N31° to 57°W. This trend represents as a second predominant in the surface structural of the geological map Fig. (80), the length of this trend 37.02% and its number 39.29% of all faults detected Table (5). The EW faults cut the NW faults, so the EW fault sets are younger than the NW fault sets (Hassan 2008).

The NW-oriented faults in the northern Eastern Desert and in the Cairo-Suez district were attributed to the Gulf of Suez-Red sea fault trend (e.g. Youssef and Abdel Rahman, 1978; Meshref, 1990, that were originated in the late Oligocene (e.g. Foly, 1941; Farag and Ismail, 1955, 1959) or in the Early Miocene (e.g. Moustafa, 1996). The NW striking depression, 60-80km wide and about 500km long (Garfunkel and Bartov, 1977).

WNW-ESE (Najd trend):

The WNW trend comprises all lineaments trending N61° to 77°W. This set includes the number of faults about 16.88% (Table 4), their length variation between "1.11"km to 5.55km. This trend represented as a third predominant structures in geological map Fig (80).

Rabie and Ammar (1990) considered this trend as an old deep-seated trend which has been reactivated many times. Dynamically, the WNW-ESE trend is interpreted by Meshref and El Sheikh (1973) and Meshref (1990) as due to the shear couple that affected the Red sea region.

NNW-SSE trend:

The NNW trend includes faults oriented from 12° N to 29° W. This trend appears as first predominant fault trend in geological map where attains 39.59% and 28.57% of the total length and number respectively Table (5), while it appear in the Landsat image as the third predominant one Fig (79).

The left lateral NNW-SSE shear, which dominates the Eastern Desert, is called G. Atalla trend by El Gaby et al., (1988). The trends of the gravity anomalies in the Gulf of Suez region are aligned along NNW-SSE trend, associated with the Miocene and post Miocene opining of the Red Sea and Gulf of Suez Markis et al., (1988). From the Upper Miocene to Quaternary, active tectonics especially these NNW-SSE lines helped further developments of the Red sea graben and Gulf of Suez El Shazly, (1966).

NE-SW trend:

The NE trend includes faults oriented from 32° N to 60° E. This trend appears as fourth predominant fault trend in the landsat image where attains 11.32% and 11.69% of the total length and number respectively, Table (4). This trend appears as minor trend in geological map.

El Shazly, (1966) explained the NE-SW structural trend as a transversal factures to the major along which huge plutons were emplaced. Meshref (1971 and 1990) interpreted the NE-SW and NW-SE trends to represent one of the two vertical shear fractures resulting from a northern compression by the end of the mountain building stage and post Orogenic transitional stage.

Table (4): Summary of the length-number ratio of lineaments detected from landsat image.

Trend	Length	L%	Number	N%
NW	146.15	23.62	52	22.52
WNW	100.27	16.13	39	16.88
EW	77.33	12.65	22	9.52
NNW	75.48	12.25	32	13.85
NE	70.3	11.32	27	11.69
ENE	59.57	9.68	25	10.82
NNE	58.83	8.93	19	8.23
NS	33.67	5.42	15	6.49
Total	621.6	100	231	100

obeikan.com

Table (5): Summary of the length-number ratio of faults detected from geological map for regional study area

Trend	Length	L%	Number	N%
NNW	215	39.59	16	28.57
NW	201	37.02	22	39.29
WNW	42	7.73	5	8.93
ENE	26	4.79	5	8.93
EW	22	4.05	4	7.14
NE	21	3.87	2	3.57
NS	16	2.95	2	3.57
Total	543	100	56	100

obeikan.com

L %							
NW	WNW	EW	NNW	NE	ENE	NNE	NS
23.62	16.13	12.65	12.25	11.32	9.68	8.93	5.42

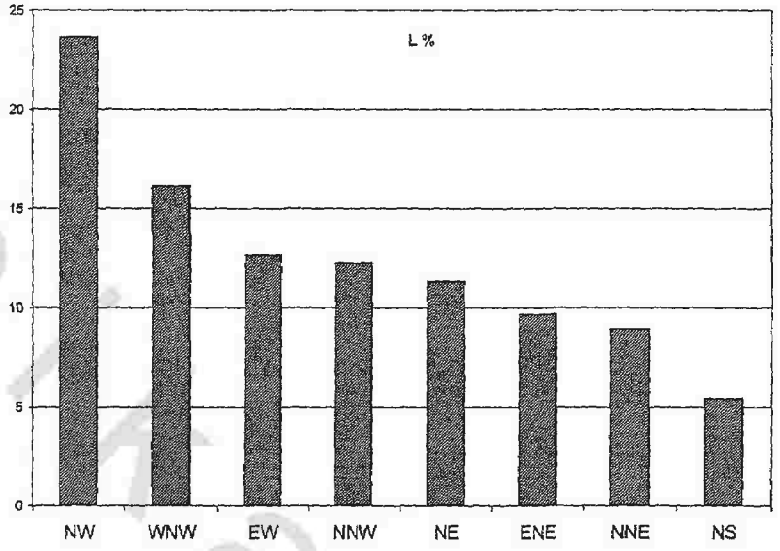

N %							
NW	WNW	EW	NNW	NE	ENE	NNE	NS
22.52	16.88	9.52	13.85	11.69	10.82	8.23	6.49

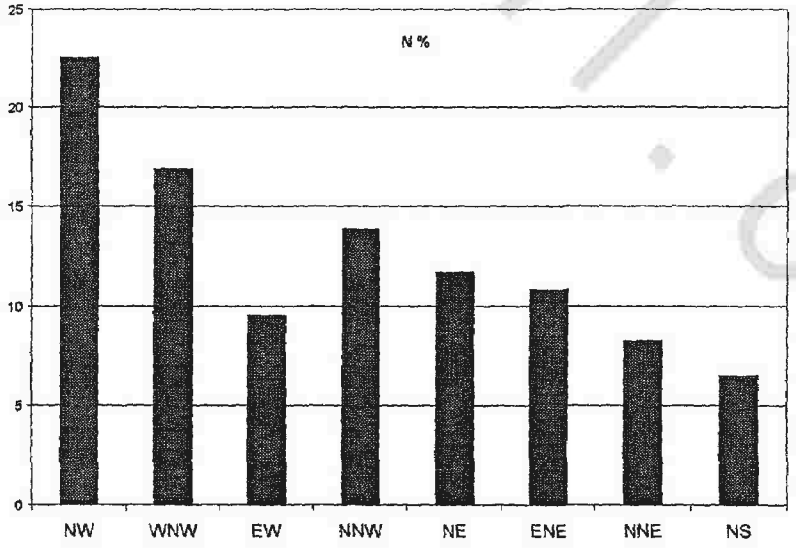

Figure (79): Histogram showing the structural trends of lineaments traced from ETM+ image.

L %						
NNW	NW	WNW	ENE	EW	NE	NS
39.59	37.02	7.73	4.79	4.05	3.87	2.95

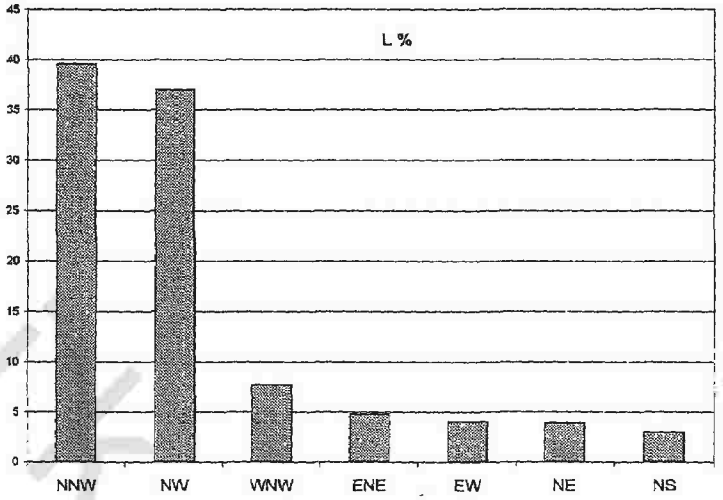

N %						
NNW	NW	WNW	ENE	EW	NE	NS
28.57	39.29	8.93	8.93	7.14	3.57	3.57

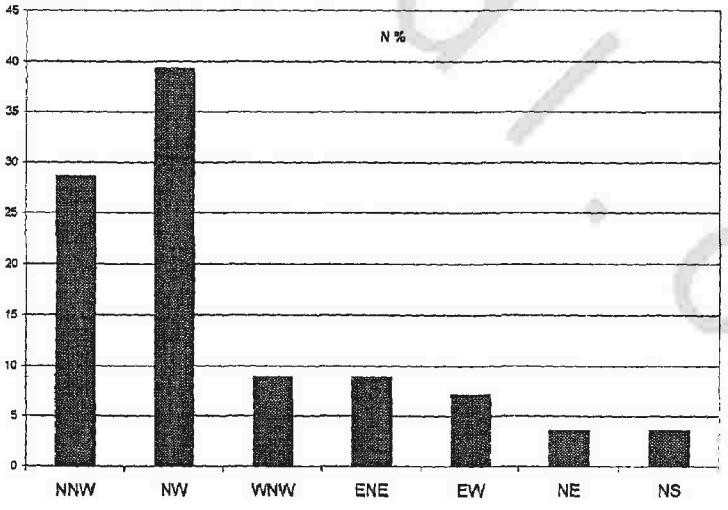

Figure (80): Histogram showing the structural extracted from geological map.

IV. 7. Fault elements detected from magnetic interpretation

Aeromagnetic maps generally show broad, low frequency anomalies resulting from relatively deeper and older structures, as well as high frequency local anomalies that reflect shallow tectonic features. Thus regional magnetic maps are of vital importance in studying older regional basement tectonics, while residual magnetic maps are important in minerals exploration and for delineating shallow tectonics associated with them.

The fault elements map reveals that the southern part of the study area is characterized by the NE major trend formed major structural horst and grabens, while central area is characterized by the prominence of NW trend. The EW trends intersected the area from its northern side.

The qualitative interpretation for the total intensity magnetic map of regional study area show the zones of maximum gradients of more dense contour lines as a locating of a probable major fault zones. As well as the direction of the downthrown of faults is taken as the direction of decreasing values of the contours. In this way fault elements were determined as shown in Fig. (81), these fault elements were analyzed and statistically studied and then plotted on a histogram diagram to illustrate the major fault trends Fig. (82), the predominant trends of faults include four sets, their orientation are N-E, N-W, NNW and E-W direction. Besides the minor fault trends are also present. The length and number percentage are tabulated in Table (6).

NE-SW trend:

The NE oriented faults are characterized by their long lengths, about 29.75% of the total length and 28.57% of the total

number of all structural faults Table (6). This trend represents as a first predominant in the subsurface structural map Fig. (82). El Shazly, (1966) explained the NE-SW structural trend as a transversal factures to the major along which huge plutons were emplaced. Meshref (1971 and 1990) interpreted the NE-SW and NW-SE trends to represent one of the two vertical shear fractures resulting from a northern compression by the end of the mountain building stage and post Orogenic transitional stage. Abu El-Ata (1988), stated that the NE trend resulted from a main stress trending to the northwest caused by the continental separation between Africa and Asia and the plate convergence from Europe to Asia, that produced the Syrian arc of folds and faults.

NW-SE trend:

The NW oriented faults are characterized by their long lengths, about 22.98% of the total length and 21.43% of the total number of all structural faults (Table 6). This trend represents as a second predominant in the subsurface structural map. The NW trend generated from a main stress directing to the southwest, due to the plate collision between Europe and Asia and the Oceanic rifting between Africa and Asia that resulted the Red Sea system of faults and folds Abu El-Ata (1988).

According to Nakhla (1982) geophysical studies on Cairo-Suez district indicate that, the NW oriented faults are believed to be the deepest comparable other fault sets. The basaltic sheets in the north and south of Wadi Akheider and both sides of Wadi Noaat in the El Galala El Bahariya were extruded through a number of the NW oriented faults Abdalla (1993). Also the basaltic sheets in the south of Gabal Abu-Treifiya were extruded

through a number of the NW oriented faults Hassan (2008).

NNW-SSE trend:

This trend appears as third predominant fault trend where attains 16.20% and 17.86% of the total length and number respectively.

The left lateral NNW-SSE shear, which dominates the Eastern Desert, is called G. Atalla trend by El Gaby et al., (1988). The trends of the gravity anomalies in the Gulf of Suez region are aligned along NNW-SSE trend, associated with the Miocene and post Miocene opining of the Red Sea and Gulf of Suez Markis et al., (1988). From the Upper Miocene to Quaternary, active tectonics especially these NNW-SSE lines helped further developments of the Red sea graben and Gulf of Suez El Shazly, (1966).

E-W trend:

The Mediterranean trend is referred to in the literatures as Tethyan trend (Said, 1962). This trend produced from a main stress orienting to the south, due to the plate divergence between Africa and Asia and the sea-floor spreading within the Mediterranean Sea that initiated the Mediterranean Sea system of faults and folds Abu El-Ata (1988). This trend appears as fourth predominant fault trend where attains 15.21% and 14.29% of the total length and number respectively. El Shazly, (1966) concluded that the E-W is the oldest tectonic trend affecting the Egyptian basement rocks where it started by the late geosynclinal stage during the Precambrian orogeny.

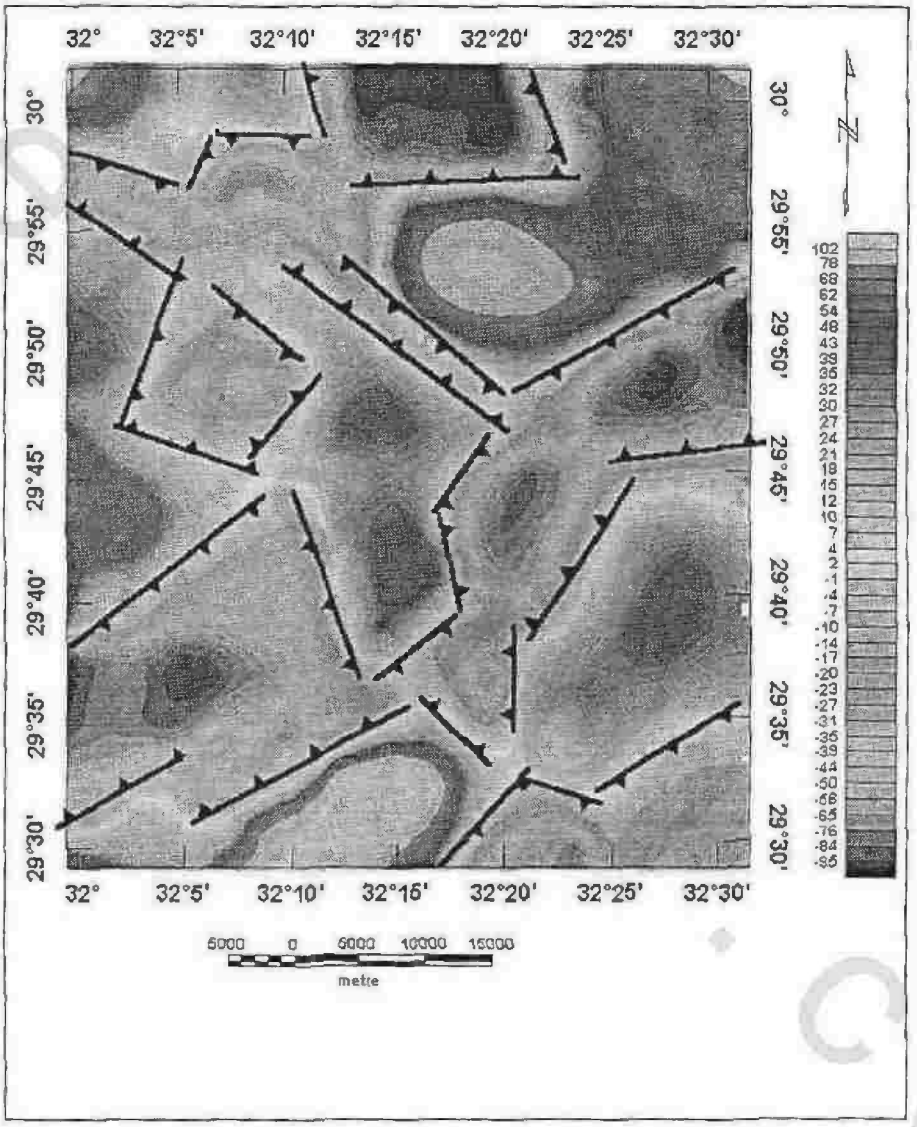

Figure (81): Fault elements dissecting the study area from magnetic interpretation.

Table (6): Summary of the length-number ratio of faults detected from magnetic anomalies map.

Trend	Length	L%	Number	N %
NE	90	29.75	8	28.57
NW	69.5.	22.98	6	21.43
NNW	49	16.20	5	17.86
EW	46	15.21	4	14.29
ENE	26.5	8.76	2	7.14
WNW	8.5	2.81	1	3.57
NS	8	2.64	1	3.57
NNE	5	1.65	1	3.57
Total	302.5	100	28	100

L %							
NE	NW	NNW	EW	ENE	WNW	NS	NNE
29.75	22.98	16.20	15.21	8.76	2.81	2.64	1.65

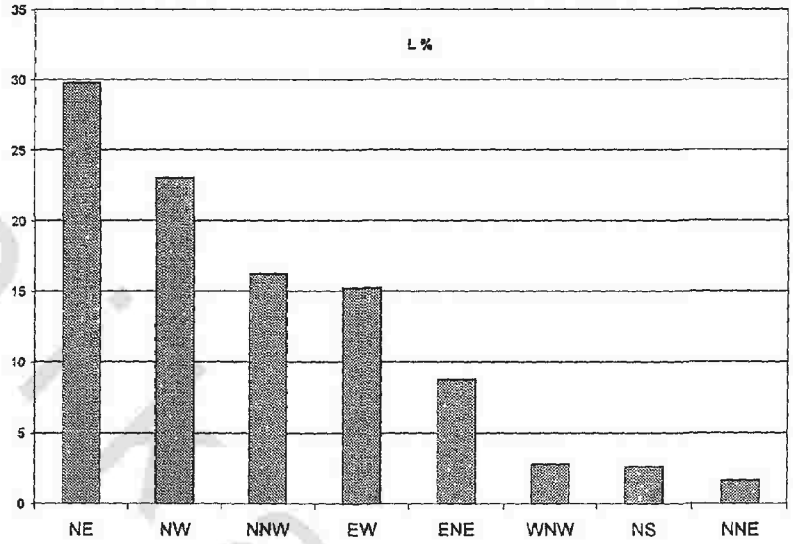

N %							
NE	NE	NE	NE	NE	NE	NE	NE
28.57	21.43	17.86	14.29	7.14	3.57	3.57	3.57

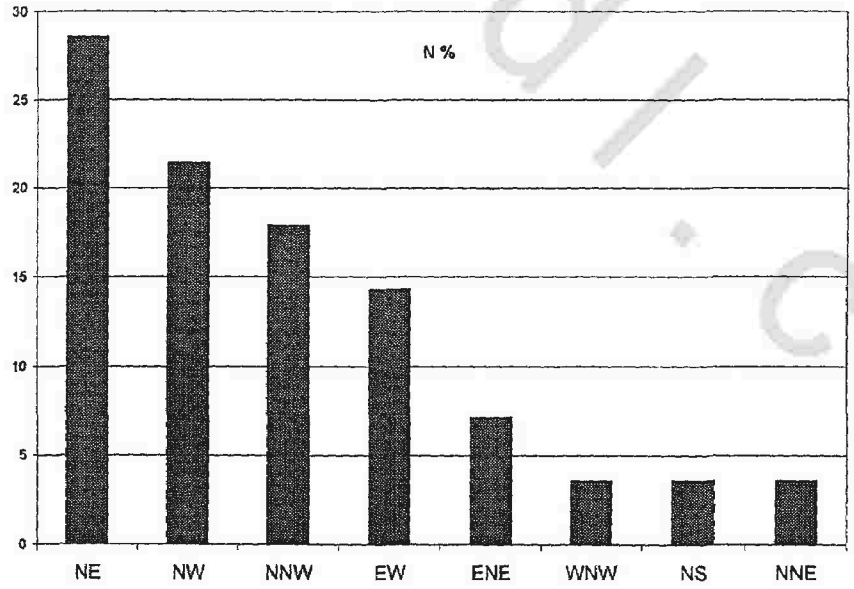

Figure (82): Histogram showing the main structural trends extracted from magnetic map.

VI. 8. Integration between geophysical and remote sensing data

The inspection of the magnetic anomaly map of the study area shows that, the shape of shore line of the western side o f the Gulf of Suez controlled by the subsurface faults. The fault system has trends NE that affected on the major part of the shore line in the studied area.

The correspondence and correlation between the structural pattern prevailed in both surface (geological map) and subsurface available data showed that, the F1, F2 and F3 which detected from them have the same extension which indicate that these faults are active fault (risk area) Fig (83).

The close correlation between different trends interpreted from magnetic, geological maps and Landsat image Fig (84) indicates that, the magnetic anomalies reflect rather well the important directions that were detected from Landsat image. These give an indicator that, the liners observed on Landsat imagery are not solely related to surface fault fracture patterns but often reflect basement weakness zones and deep seated structural trends. There are some differences in the arrangement of effective trends for both surface and subsurface data (Table 7 and Fig. 85).

These differences are related to the fact that, 1) the sedimentary cover assumed as non magnetic, and the magnetic measurements are related mainly to the basement rocks. 2) Faults detected from magnetic anomalies are mainly due to basement structural where those of Landsat imagery may reflect at least in part shallower structures. 3) It is not always true that all basement structures are transmitted into the overlying sedimentary cover. This depends on their magnitude and duration of the stress field and possibility of rejuvenations.

There are some major tectonic trends (NW, WNW, WNW and NNW) interpreted from magnetic, geological data as well as surfaces lineaments images. This may suggest that both the basement and the overlying sediments had been affected by these tectonic trends. It had probably reactivated during the geological times. Some fault trends which appear in the magnetic map, have no indication to be present on the surface images. This type of faults may be covered and could not be appear on the Landsat images.

obeikandl.com

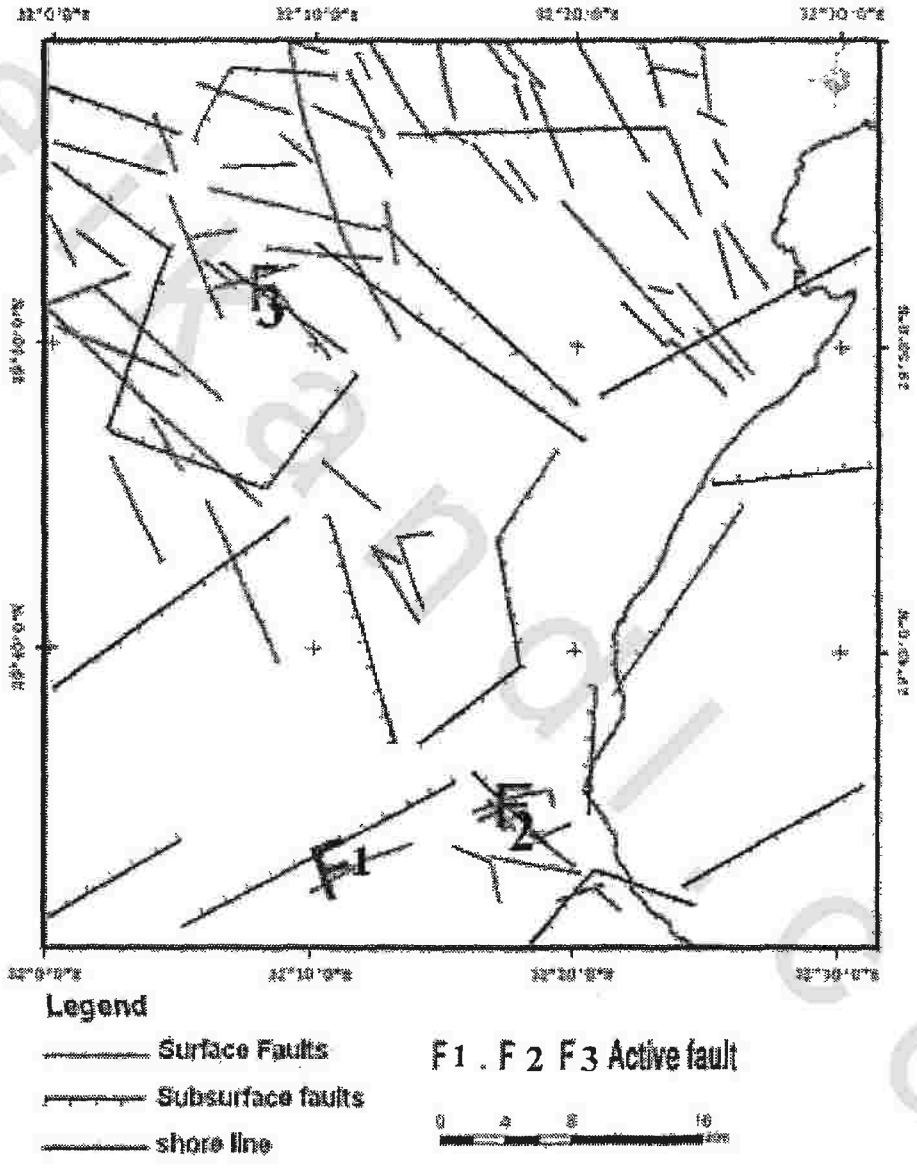

Figure (83): Active faults map of the study area.

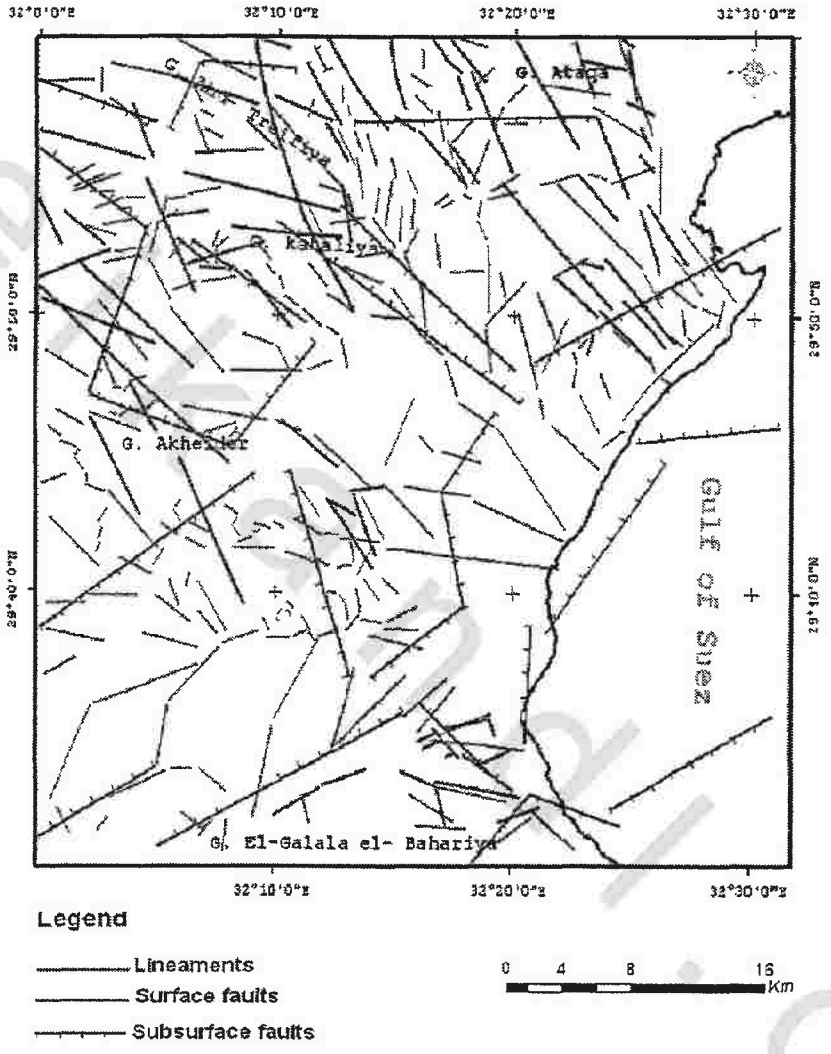

Figure (84): Extracted lineaments and faults by using Landsat ETM+ and magnetic data.

Table (7): Interpreted trends for Landsat, geological and magnetic maps as arranged in decreasing orders of predominance.

Maps / Orders	Landsat map	Geological map	Magnetic map
1st order	NW	NW	NE
2nd order	WNW	NNW	NW
3rd order	NNW	WNW	NNW
4th order	EW	ENE	EW
5th order	NE	EW	ENE

obeikan.com

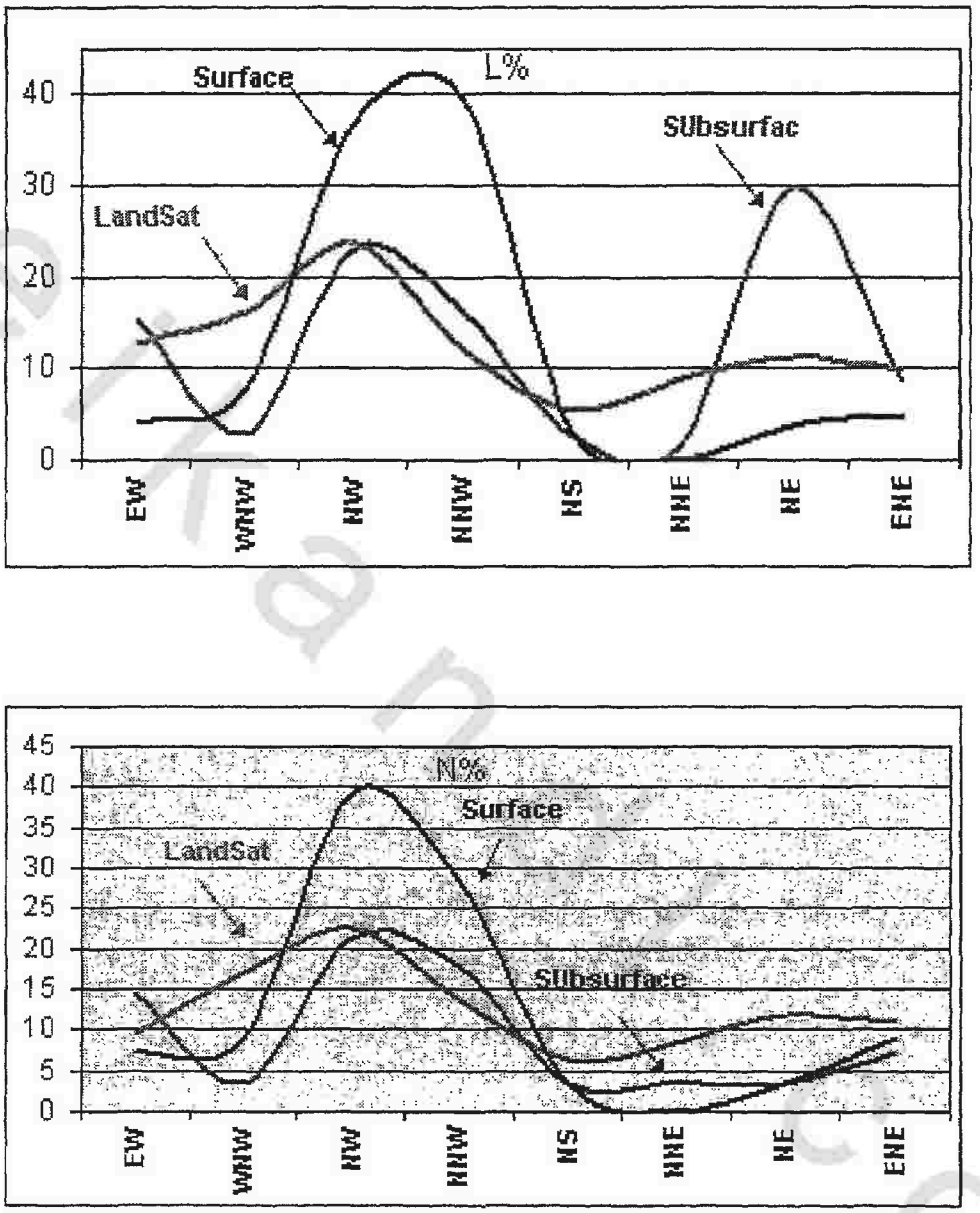

Figure (85): Frequency distribution curves of lineaments and faults by using Landsat ETM+, surface and magnetic data.

CHAPTER VII
GIS AND ENVIRONMENTAL HAZARD

VII. 1. Introduction

Geographic Information System (GIS) is a computer-based system capable of capturing, storing. Manipulating, analyzing and displaying the geographical information. Cowen (1988) defined it as" a decision support system involving the integration of spatially referenced data in a problem solving environment".

GIS is designed for collection and storage and analysis of objects and phenomena where geographic location is an important characteristic or critical to the analysis. It enables the users to work quickly with the data, especially when the quantity of data involved is too large to be handled manually. These data may exist in different formats. Spatial and non-spatial (attribute) data, raster and vector data and digital or analog data formats. In the present work the Landsat ETM+ images and different types of digitized maps represent the spatial data format. Information about a geologic setting represents the non spatial data format.

Spatial elements can be represented in two models: Vector and Raster. In the vector model, the spatial locations of features are defined on the basis of coordinate pairs. These can be discrete, taking the form of points linked together to form discrete sections of line, linked together to form closed boundaries encompassing an area (polygon data). The data model used by the software, like Arc/Info, Arc View is Vector model. In raster model, one or group of cell/grid/pixel depending upon the grid resolution represents spatial elements.

VII. 2. Capabilities of Geographic Information System

Geographic information systems abbreviated to GIS are computer based system that provides the following four sets capabilities to handle geo-referenced data:
1-Data acquisition and pre-processing (input data tables and digital maps with its database).
2-Data management, storage and retrieval
3-Manipulation and analysis.
4-Product generation (output).

VII. 2. 1. Data acquisition and pre-processing (data input)

Data input is the procedure of encoding data into a computer-readable form and writing the data to the GIS database. Data entry were usually the major bottleneck in implementing a GIS where the creation of an accurate and well-document database is critical to the operation of a GIS. The data used in this study are in two types:
1-Spatial data that represent the geographic location of features.
(a) Points are represented by water wells (Fig.73).
(b) Lines are represented by lineaments, faults, drainage and roads in chapters 1 and 6, active faults (Fig. 83). and drainage basin (Fig. 88)
(c) Polygon is represented by land suitability map (Fig. 89).
2-Non spatial attribute data that provide descriptive information like the name of geologic unit, abbreviation, description of these units, code of color or code of definition of any element. During data input the spatial and attribute data must be entered and correctly linked.

Types of data entry

I-Keyboard entry procedure (used for most attribute data).
2-Coordinate geometry (used to enter land record information) to obtain a very high level of precision by

entering the actual survey measurements.
3- Manual digitizing (by using digitizing table or on screen) by tracing the feature from a pre-fixed maps or scanned maps.

GIS techniques have been used in this study to create and built up a vector layers for formed the data in new form using Arc Map (Version 9.1)

The first step in this works are (Digitizing), the manual digitizing on screen methods of data input is used to built up vector layers for all different rock unites in the area under studying. These maps are input into the computer by scanning process and by using ERDAS Imagine software (V. 9.1) have been rectified these maps.

GIS software Arc Map (V. 9.1) is used for digitizing process by tracing all rock units by drawing tool polygon, and create attribute include on the data related to all these polygons include list of rock name, and descriptive information; and building topology for each layer, where each rock unit represented a vector layer, after digitizing process are finishing all layers can he opened together.

VII. 2. 2. The Data Management

The data management includes those functions needed to store and retrieve data from data base. The methods used to implement these functions affect how efficiently the system performs all operations with the data. Organizing the data into computer readable files, data structure, the way the files can be related to each other, the way the data can be retrieved and the speed of the retrieval operation are the most important steps in this respect.

VII. 2. 3. Data output

Data output is the procedure by which information from the GIS is presented in a suitable form to the user. Data are output either hardcopy, or softcopy.

1-Hardcopy output is permanent means of display (the information is printed on a paper).
2-Softcopy output is the format of storing the output on electronic media (compact disk, floppy desk, etc.).

VII. 2. 4. Data manipulation and analysis

In the present study the data analysis includes, the analysis of Digital Elevation Model (DEM), slope, and shaded relief (chapter 6). The intersect process used to correlated between the geological map compiled from previous data (chapter 3). The overlaying process used to the structure map (chapter 6).

VII. 3. Enviromental hazard

Enviromental geology is the branch of geology that deals with the application of geological science in enviromental issues. Resources , natural hazards man-made hazards and hazard assesment are the main topics in enviromental geology (El-Sawy, 2005).

Natural hazards are naturally occurring processes that may be dangerous to human life and properties. Volcanic eruptions, earthquackes, hurricanes, floods, mass wasting , and pollution are all examples of natural hazards. Human pollution continues to increase, and there is a need to develop enviromentally sound stratiges to minimize the loss of life and property damage from hazards , espicially in urban area (keller,2002)

VII. 3.1. Seismic activity

Although seismic activity in Egypt is considered low, but seismic risk is considerably high. This is due to the fact that most the earthquakes occur close to overpopulated

cities and villages, coupled with old methods of construction and poor construction practice. Soil characteristics in different localities in Egypt and their impact on seismic wave attenuation and modification are important parameters that control earthquake risk (El Baz and Raid 2002). Some earthquake events took place in and around the study area Fig (86). Table (8) represents 217 earthquake events recorded in the study area. The events (1 and 24) recorded inside the area of magnitude 4.2 and 4.1 respectively and located near the fault F3 and F4 which indicates that this faults is an active faults Fig (87). Therefore, the constructions must be made far away from the fault zone with a distance at least 0.5 km.

VII. 3.2. Floods as a natural hazard

Natural flooding processes can also become hazards when land use changes such as urbanization or deforestation affected by natural processes, causing flooding (El-Sawy, 2005).

To avoid the destructive impacts of the flooding in the studied area and to get benefits of the flooding water as it is urgently needed dams in the upstreams as well at the mouths of each basin have to be constructed, Fig (88) .

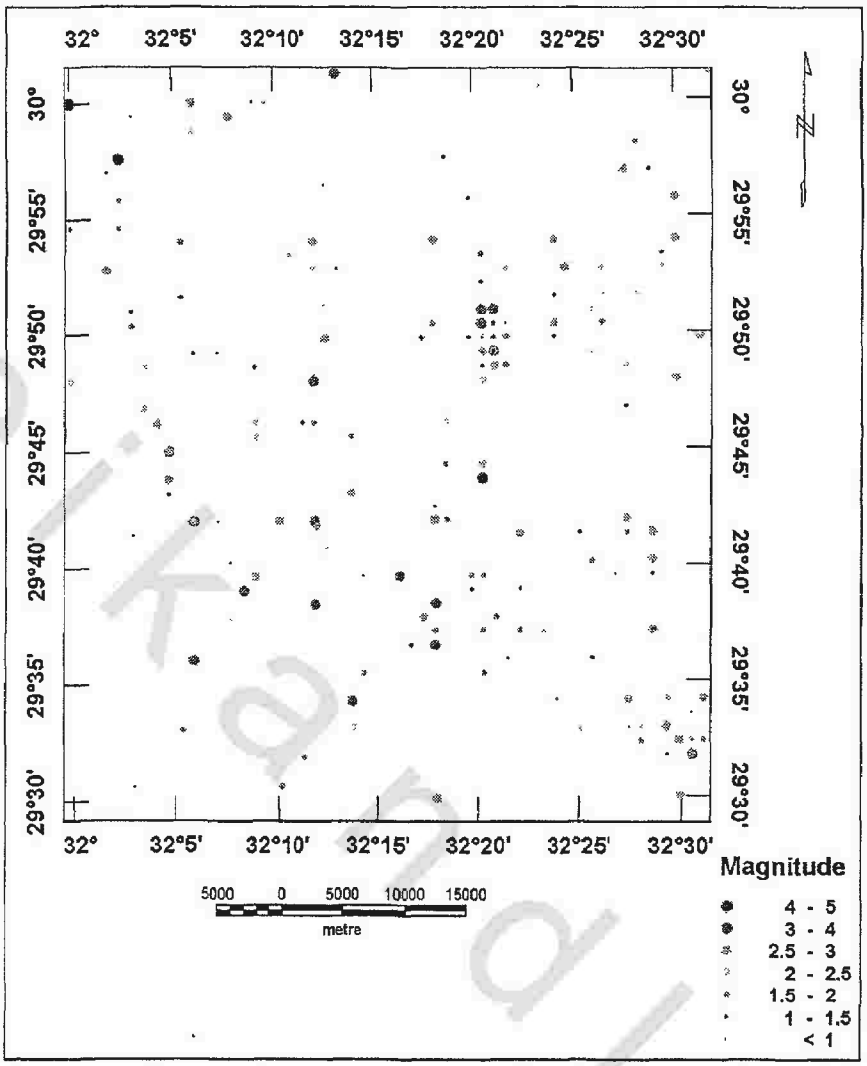

Figure (86): Distribution of the earthquake events that took place in the study area (after El Baz and Riad, 2002).

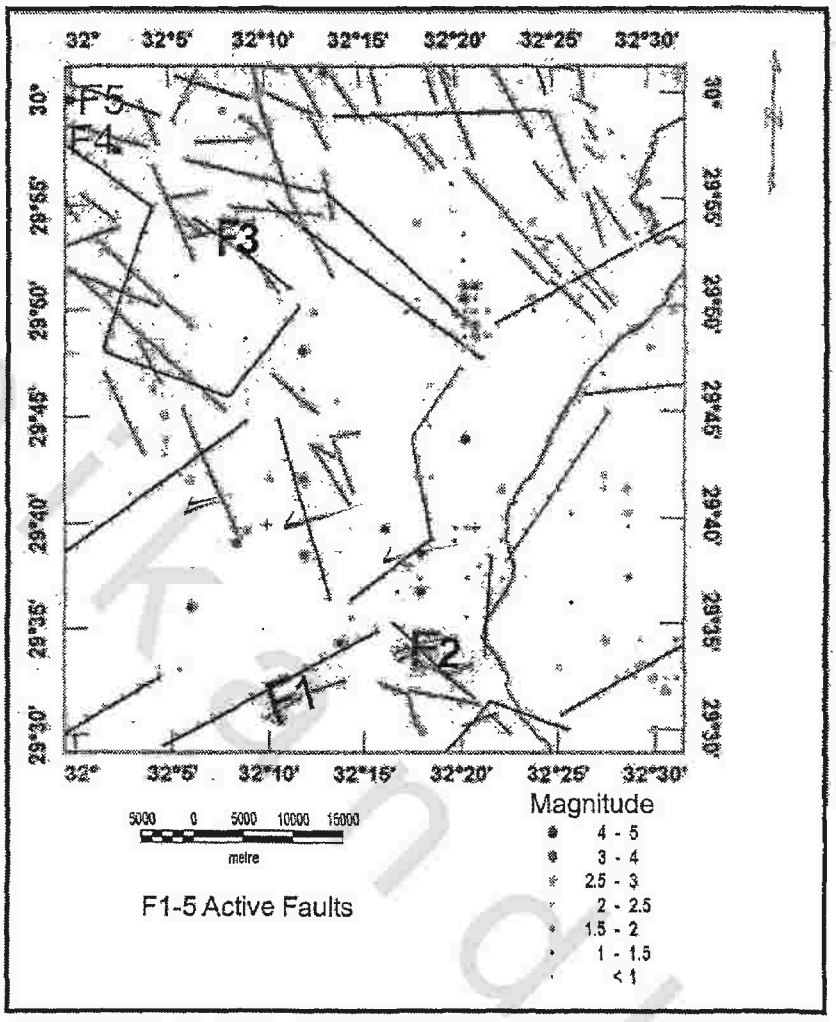

Figure (87): Active faults extracted from distribution of the earthquake events that took place in the study area

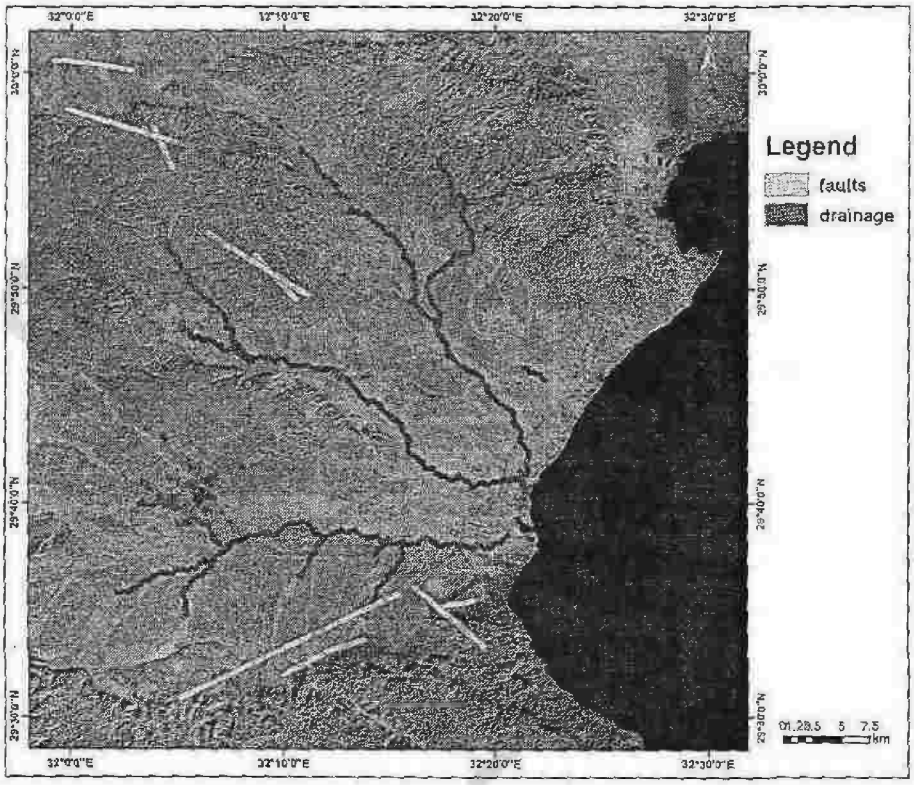

Figure (88): Risk map showing the buffer zone of active faults and drainage basin.

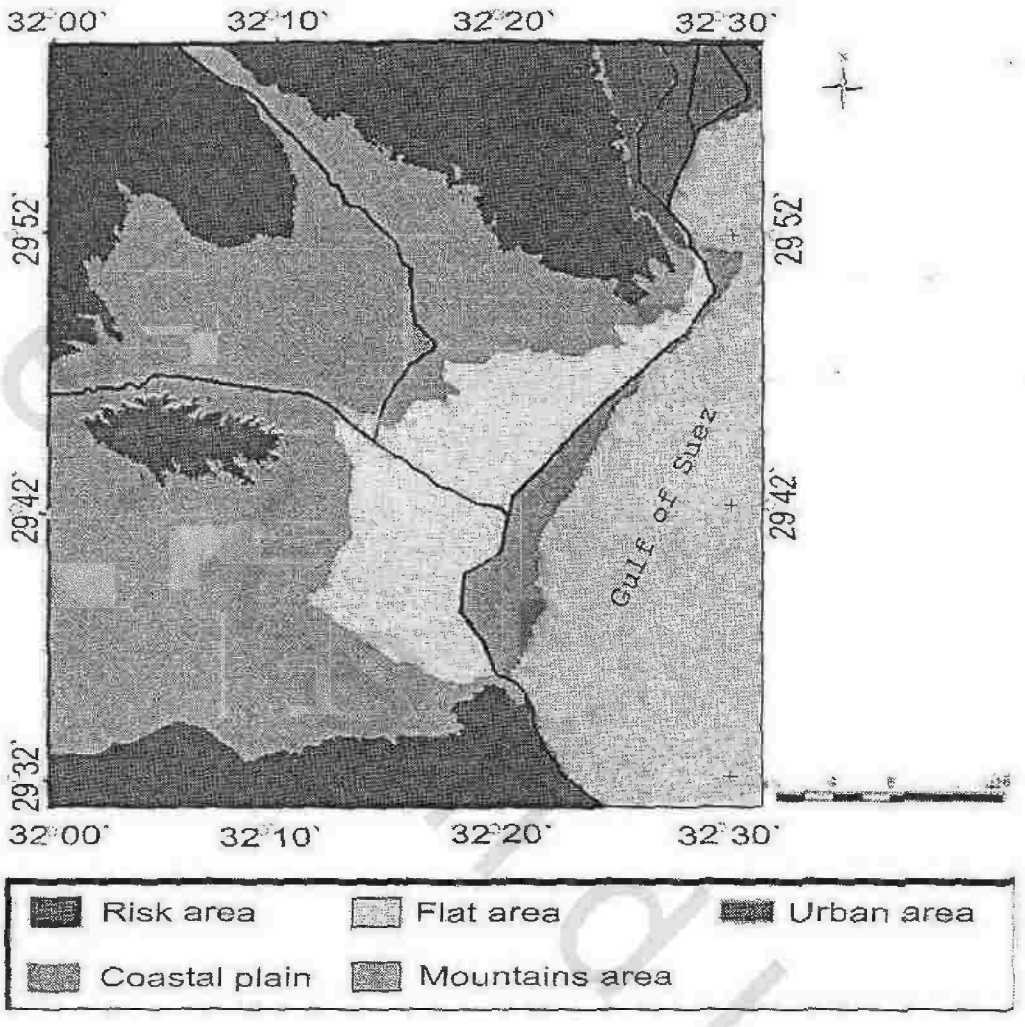

Figure (89): Land suitability map of the study area.

VII. 4. Conclusion and results

GIS analysis has been applied in three chapters in this thesis, and the result is generating a land suitability map of the study area depending upon the database which has been available such as geologic maps, structural maps, geomorphological maps, geoelctrical resistivity survey, risk maps, and active faults.

According the land suitability map (Fig.89), the study area can be classified into five main units, each unit is characterized by specific geotechnical features, and the following is a brief description for each unit:

First unit: (risk area) This unit can be avoided from any constructions and engineering purposes, because it consisting of tracks of the flood plains and active faults.

Second unit: This unit represents the coastal plain, can be utilized for construction a new seaport, tourism places and beach resort.

Third unit: (flate area) This is the best and preferred unit for construction and engineering purposes, this unit is flatness and consisting of Quaternary wadi fill deposits of sand and gravel horizontal layers. We should note the any infrastructure must be fare from the fault plaine and the flood zones to be save.

Fourth unit:(mountains area) This unit can be avoided from any constructions and engineering purposes, because it represents the western mountains area of the study area, which can be used as an open areas such gardens, playgrounds …etc.

Fifth unit: This unit represents the urban area.

The land suitability map shows that area is of great importance in sustainable development. It has a fantastic shore, well whether and archeological places for both internal and external tourism. The mountains and the wadies are a suitable for safari tourism.

Table (8): Description of the earthquake events that took place in the study area (after Elbaz and Riad, 2002).

No.	Lat.	Long.	Depth	Distribution.	No.	Lat.	Long.	Depth	Mag.
1	30	32	20	4.2	29	29.57	32.23	25	3.8
2	29.5	32.3	20	3	30	29.61	32.3	6	3.5
3	29.99	32.13	2	2.9	31	29.64	32.3	6	3.4
4	29.64	32.2	20	3.4	32	29.93	32.5	6	2.9
5	29.75	32.08	17	3.6	33	29.6	32.1	20	3.3
6	29.95	32.46	7	2.7	34	29.7	32.17	6	2.9
7	29.8	32.2	38	3.37	35	29.75	32.08	3	2.9
8	29.5	32.5	22	2.89	36	29.66	32.15	18	2.9
9	29.8	32.2	21	3.34	37	29.77	32.07	5	2.7
10	29.5	32.5	20	2.9	38	29.84	32.05	18	2
12	30	32.1	38	2.5	39	29.63	32.13	15	2.5
13	29.9	32.4	21	2.9	40	29.7	32.1	26	2.2
14	29.9	32.2	0	2.82	41	29.67	32.48	14	3
15	29.7	32.3	9	2.72	42	29.98	32.1	18	2.4
16	29.9	32.4	20	2.85	43	29.74	32.31	5	1.6
17	29.7	32.2	0	3.31	44	29.74	32.34	23	2.3
18	30	32.1	29	2.9	45	29.91	32	16	1.1
19	29.7	32.1	1	3.25	46	29.86	32.09	16	1.1
20	29.9	32.3	13	2.76	47	29.76	32.23	10	1.8
21	29.9	32.5	22	2.8	48	29.82	32.1	8	1.2
22	29.66	32.27	13	3.1	49	29.83	32.52	26	2.7
23	29.55	32.23	10	2.1	50	29.88	32.41	9	2.9
24	29.96	32.04	17	4.1	51	29.63	32.29	1	2.8
25	29.69	32.20	5	2.8	52	29.84	32.4	16	2.8
26	29.73	32.34	25	4.3	53	29.8	32.5	18	2.9
27	29.83	32.21	6	2.7	54	29.7	32.46	18	2.6
28	29.62	32.48	3	2.8	55	29.9	32.09	30	1.9

56	29.91	32.33	17	2.3	86	29.82	32.43	8	2.3
57	29.6	32.36	15	1	87	29.88	32.49	15	2.4
58	29.73	32.08	25	2.6	88	29.55	32.09	15	1.7
59	29.57	32.46	21	3	89	29.94	32.21	10	0.8
60	29.55	32.46	14	0.9	90	29.83	32.36	20	1.9
61	29.72	32.23	21	2.6	91	29.85	32.35	9	2.7
62	29.57	32.49	9	2.3	92	29.87	32.34	10	1.3
63	30.02	32.53	22	1.9	93	29.86	32.4	15	1.2
64	29.84	32.18	18	2.1	94	29.89	32.34	20	1.7
65	29.97	32.47	15	1.7	95	29.88	32.2	5	2.2
66	29.69	32.48	18	2.9	96	29.84	32.34	4	1.3
67	29.88	32.03	30	3	97	29.88	32.44	13	2.3
68	29.72	32.08	8	1.3	98	29.93	32.33	3	1.3
69	29.82	32.12	18	0.8	99	29.89	32.18	4	2.4
70	29.69	32.37	4	2.8	100	29.54	32.47	18	1.8
71	29.85	32.43	2	2.5	101	29.83	32.29	6	1.6
72	29.62	32.3	15	1.9	102	29.95	32.48	17	1.5
73	29.55	32.42	4	2.4	103	29.84	32.44	5	1.7
74	29.81	32.46	19	2.3	104	29.77	32.19	10	1.5
75	30.01	32.39	15	2.1	105	29.81	32.15	34	1.2
76	29.99	32.05	10	0.1	106	29.77	32.2	0	1.6
77	29.77	32.31	14	2.4	107	29.86	32.44	3	2.5
78	29.85	32.35	19	1.4	108	29.51	32.05	18	1
79	29.7	32.31	15	1.1	109	29.66	32.24	7	0.9
80	29.71	32.3	22	0.8	110	29.53	32.51	16	3.4
81	29.84	32.3	18	2	111	29.57	32.52	4	2.8
82	29.88	32.36	17	2.2	112	29.54	32.51	14	2.5
83	29.63	32.31	10	1.5	113	29.53	32.51	11	2.2
84	29.66	32.27	15	0.7	114	29.55	32.49	6	2.7
85	29.7	32.12	2	0.8	115	29.56	32.51	18	1

116	29.54	32.52	14	1.7	145	29.78	32.46	22	1.3
117	29.54	32.51	11	0.4	146	29.69	32.46	10	1.7
118	29.53	32.49	15	0.6	147	29.53	32.19	14	1.9
119	29.54	32.51	12	1	148	29.53	32.51	14	2.7
120	29.55	32.47	15	2.3	149	29.66	32.34	16	1.6
121	29.54	32.5	6	3	150	29.93	32.04	18	2
122	29.62	32.37	4	1.7	151	29.96	32.31	11	1.3
123	29.59	32.34	14	1.9	152	30.02	32.22	24	3.2
124	29.86	32.44	19	2.2	153	29.85	32.35	18	3.1
125	29.77	32.15	11	2.4	154	29.86	32.33	17	2.5
126	29.63	32.35	10	1.9	155	29.96	32.31	30	0.9
127	29.66	32.33	22	1.7	156	29.76	32.15	16	2.4
128	29.59	32.24	23	1.7	157	29.8	32	10	2.3
129	30	32.15	18	1	158	29.65	32.14	21	3.3
130	29.66	32.45	18	0.6	159	29.83	32.34	4	2.1
131	29.63	32.31	12	2.4	160	29.83	32.33	4	1.5
132	29.65	32.37	6	1.5	161	29.65	32.33	13	1.5
133	29.51	32.17	7	1.9	162	29.82	32.34	4	1.9
134	29.85	32.05	20	1.3	163	29.81	32.34	4	1.5
135	29.62	32.34	12	1.8	164	29.67	32.43	4	1.7
136	29.57	32.4	9	1	165	29.95	32.03	15	0.5
137	29.67	32.13	20	0.5	166	29.81	32.35	3	2.6
138	30	32.16	16	2.1	167	29.83	32.29	15	0.8
139	29.6	32.43	8	1.4	168	29.78	32.06	0	2.2
140	29.91	32.04	10	1.7	169	29.61	32.28	17	1.6
141	29.69	32.05	10	0.8	170	29.82	32.34	8	3
142	29.86	32.47	10	2.3	171	29.83	32.34	10	1
143	29.62	32.48	20	1.2	172	29.82	32.34	4	2.5
144	29.62	32.39	6	2.3	173	29.83	32.34	11	1.6

174	29.84	32.34	10	1.1	196	29.83	32.35	8	1.6
175	29.66	32.48	19	1.4	197	29.84	32.36	10	0.9
176	29.66	32.48	19	1.4	198	29.84	32.36	10	0.9
177	29.82	32.35	5	3.2	199	29.83	32.34	5	2.2
178	29.82	32.35	5	3.2	200	29.83	32.34	5	2.2
179	29.83	32.35	6	1.6	201	29.82	32.35	4	3.6
180	29.83	32.35	6	1.6	202	29.82	32.35	4	3.6
181	29.82	32.35	8	1.6	203	29.84	32.35	14	1.3
182	29.82	32.35	8	1.6	204	29.84	32.35	14	1.3
183	29.81	32.36	3	1.6	205	29.82	32.34	10	2.2
184	29.81	32.36	3	1.6	206	29.82	32.34	10	2.2
185	29.82	32.34	4	2.6	207	29.83	32.35	3	1.6
186	29.82	32.34	4	2.6	208	29.83	32.35	3	1.6
187	29.8	32.34	4	2.6	209	29.82	32.35	4	2.2
188	29.8	32.34	4	2.6	210	29.82	32.35	4	2.2
189	29.8	32.34	8	2.4	211	29.82	32.35	4	1.5
190	29.8	32.34	8	2.4	212	29.82	32.35	4	1.5
191	29.85	32.34	8	3.1	213	29.7	32.31	15	2
192	29.85	32.34	6	3.1	214	29.81	32.06	5	2.1
193	29.84	32.34	6	3.1	215	29.68	32.21	4	2.3
194	29.84	32.34	4	3.1	216	29.61	32.28	5	1.3
195	29.83	32.35	8	1.6	217	29.82	32.34	4	1.9